Journal of Southeast University (English Edition) Vol. 21, No. 3, pp. 363 – 368 Sept. 2005 ISSN 1003—7985

Cycle slip detection approach based on time-relative positioning theory

Yu Guorong Sheng Renjun

(College of Transportation, Southeast University, Nanjing 210096, China)

Abstract: An efficient cycle slip detection method is proposed for high precision positioning and navigation results with global positioning system (GPS), which is based on the assumption of a high sampling interval, measurement errors are so small that they can be ignored in the temporal single difference observables. And ambiguities are ordinarily equal to zero, but could be the number of cycles that have "slipped" if loss-of-lock has occurred. Therefore, cycle slips are estimated as parameters of time-relative positioning observation equations. Because the temporal single difference observables are taken at different epochs and different stations with a single GPS receiver, if time-relative positioning observation equations are linearized as that of conventional relative positioning, the design matrix will be rank defective. To obtain a stable linearization scheme, time-relative positioning observation equations are further analyzed, and the concept of virtual measurement is applied. A sample of data collected on a vehicle test shows that a cycle slip detection approach based on time-relative positioning theory can detect slips at the value of one cycle. The results also indicate if two satellites are so near to each other that they have the same equivalent to satellite-receiver geometry, cycle slip detection will be difficult and may get wrong results. Cycle slips of different satellites also affect detection by satellite-receiver geometry.

Key words: global positioning system (GPS); cycle slips; time-relative positioning; satellite-receiver geometry

Cycle slips are discontinuities of an integer number of cycles in the measured (integrated) carrier phase resulting from a temporary loss-of-lock in the carrier tracking loop of a GPS receiver. In this event, the integer counter is reinitialized which causes a jump in the instantaneous accumulated phase by an integer number of cycles. The detection and correction of cycle slips are needed if accurate positioning is to be carried out. Cycle slip detection and correction require the location of the jump and the determination of its size. It can be completely removed once it is correctly detected and identified.

Slip detection and repair still represent a challenge to carrier phase data processing even after years of research. All methods have the common premise that to detect a slip at least one smooth quantity derived from the observations must be tested in some manner for discontinuities that may represent cycle slips[1,2]. The derived quantities usually consist of linear combinations of the indifferenced or double-differenced L1 and L2 carrier-phase and possibly pseudorange observations. Examples of combinations useful for kinematic data are the geometry-free phase (a scaled version which is called the ionospheric phase delay)[1-4] and wide-lane phase minus narrow-lane pseudorange[2,4,5]. Kalman filtering is a popular method, especially for kinematic data processing where such filtering is used in the main processing stage[3,6].

Time-relative positioning is a recently developed method for processing GPS observations. By processing carrier phase observations taken at different epochs (and different stations) with a single GPS receiver, relative positioning is then obtained[7]. Because carrier phase observations are performed with the same receiver, carrier phase ambiguity is common to the two observation epochs if there is no cycle slip. The ambiguities are ordinarily equal to zero in the temporal single difference observables, but could be the number of cycles that have "slipped" if loss-of-lock has occurred. Therefore, the temporal single difference observables can be used to detect cycle slips.

1 Observable Model

The mathematical models for raw carrier phase and pseudo-range observables are

Received 2005-01-04.

Biography: Yu Guorong(1971—), male, doctor, ygr. fish@163. com.

For the L1 frequency

$$\left.\begin{aligned} R_1 &= \rho + c(\delta t_u - \delta t^s) + T + I_1 + MR_1 + \varepsilon R_1 \\ \lambda_1\phi_1 &= \rho + c(\delta t_u - \delta t^s) + T - I_1 + \lambda_1 a_1 + m\phi_1 + \varepsilon\phi_1 \end{aligned}\right\} \tag{1}$$

For the L2 frequency

$$\left.\begin{aligned} R_2 &= \rho + c(\delta t_u - \delta t^s) + T + I_2 + MR_2 + \varepsilon R_2 \\ \lambda_2\phi_2 &= \rho + c(\delta t_u - \delta t^s) + T - I_2 + \lambda_2 a_2 + m\phi_2 + \varepsilon\phi_2 \end{aligned}\right\} \tag{2}$$

where the subscripts 1 and 2 denote the GPS signals; ϕ and R are the measured carrier phase and pseudo-range; λ is carrier wavelength; ρ is the geometric range from receiver to the GPS satellite; c is the vacuum speed of light; $\delta t_u - \delta t^s$ is the offsets of the receiver and GPS satellite clocks from GPS Time; a is the ambiguity; T and I are the delays due to the ionosphere and the troposphere, $I_2 = (\lambda_2/\lambda_1)^2 I_1 = r_{12}^2 I_1 = r_{12}^2 I$; M and m represent the effect of multipath; ε represents the effect of receiver noise. Satellite and receiver hardware delays and other small effects have been ignored as they have negligible effect on data preprocessing.

From the computational point of view, the distance dependent biases have a high temporal correlation. This means that between two consecutive observation epochs the GPS signals have been affected by almost the same atmospheric propagation conditions. Hence, the temporal single difference observables (see Fig. 1) are similarly affected. The temporal single difference observation equation is

$$\begin{aligned} \lambda_1\delta\phi_1 = \lambda_1\phi_1(t+k) - \lambda_1\phi_1(t) &= [\rho(t+k) - \rho(t)] + [c(\delta t_u(t+k) - \delta t^s(t+k)) - c(\delta t_u(t) - \delta t^s(t))] + \\ \lambda_1\Delta a_1 - [I(t+k) - I(t)] &+ [T(t+k) - T(k)] + [m\phi_1(t+k) - m\phi_1(t)] + [\varepsilon\phi_1(t+k) - \varepsilon\phi_1(k)] \end{aligned} \tag{3}$$

where Δa_1 denotes cycle slips. Eq. (3) possesses two specific characteristics that differentiate it from the classical (between receivers) single-difference equation (see Fig. 2). The first characteristic is related to the temporal decorrelation of GPS errors. This mainly affects the satellite clock error (and to a lesser extent the satellite ephemeredes), which is not entirely eliminated in temporal single-difference observations because this error significantly varies between two epochs. This is due to combined observations having been taken at two different epochs, i. e., they are not taken simultaneously as they are for conventional relative positioning. The second is the elimination of carrier phase ambiguity when the temporal single difference is formed[7]. Because carrier phase observations are performed with the same receiver, carrier phase ambiguity is common to the two observation epochs if there is no cycle slip. The cycle slips, Δa_1, are ordinarily equal to zero, but could be the number of cycles that have "slipped" if loss-of-lock has occurred.

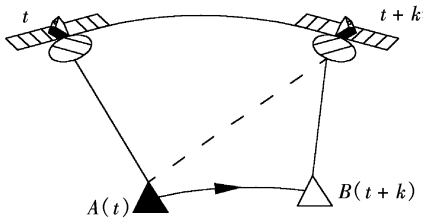

Fig. 1 Time-relative positioning

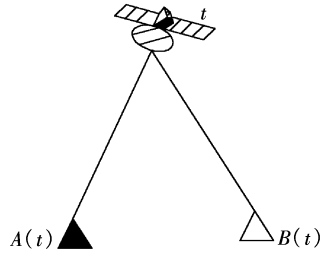

Fig. 2 Conventional relative positioning

2 Observation Equations Linearization

Regardless of surveying mode (static or kinematic) and baseline length (short, medium or long), the effects of the temporal single differenced biases and noise (i. e., atmospheric delay, satellite orbit bias, multipath, and receiver system noise) are more or less below a few centimeters in size as long as the observation sampling interval is relatively short[8]. Therefore, Eq. (3) can be simply expressed as

$$\lambda_1\phi_1(t+k) - \lambda_1\phi_1(t) = [\rho(t+k) - \rho(t)] + [c(\delta t_u(t+k) - \delta t^s(t+k)) - c(\delta t_u(t) - \delta t^s(t))] + \lambda_1\Delta a_1 \tag{4}$$

If we linearized Eq. (4) at epoch $t+k$ and t as

$$\begin{aligned} \lambda_1\phi_1(t+k) - \lambda_1\phi_1(t) &= [e_x(t+k)\delta x(t+k) - e_x(t)\delta x(t)] + [e_y(t+k)\delta y(t+k) - e_y(t)\delta y(t)] + \\ [e_z(t+k)\delta z(t+k) - e_z(t)\delta z(t)] &+ [c(\delta t_u(t+k) - \delta t^s(t+k)) - c(\delta t_u(t) - \delta t^s(t))] + \lambda_1\Delta a_1 \end{aligned} \tag{5}$$

where e_x, e_y, e_z are the satellite-receiver's direction cosines, so many unknown parameters are introduced in Eq. (5) and cause the design matrix rank defective that no stable results can be obtained. Let us consider another linearization strategy, where the virtual measurements are introduced (see Fig. 1), i. e. assume the receiver obtains a measurement sent from the satellite at the time $t+k$ while the receiver is located at the site A at the time t.

Then Eq. (4) is equivalent to

$$\lambda\phi_{t+k}^{t+k}-\lambda\phi_t^t=\lambda\phi_{t+k}^{t+k}-\lambda\phi_t^{t+k}+\lambda\phi_t^{t+k}-\lambda\phi_t^t=(\rho_{t+k}^{t+k}-\rho_t^{t+k})+(\rho_t^{t+k}-\rho_t^t)+$$
$$[c(\delta t_u(t+k)-\delta t^s(t+k))-c(\delta t_u(t)-\delta t^s(t))]+\lambda_1\Delta a_1 \tag{6}$$

Eq. (6) can be linearized as for the method of the linearization of the classical (between receivers) single-difference equation. The remaining processing consists of a standard, epoch-by-epoch, least squares adjustment with four unknown parameters: the three coordinates of the unknown station with the fourth parameter being the variation of the receiver clock error between the two epochs.

3 Cycle Slip Detection

The least squares adjustment system is

$$\boldsymbol{V}=\boldsymbol{A}\delta\boldsymbol{X}+(\boldsymbol{l}+\boldsymbol{\Delta}) \qquad \text{with power } \boldsymbol{P} \tag{7}$$

where $\boldsymbol{\Delta}$ is the vector of cycle slip, then

$$\delta\hat{\boldsymbol{X}}=-\boldsymbol{N}^{-1}\boldsymbol{U},\quad \boldsymbol{N}=\boldsymbol{A}^{\mathrm{T}}\boldsymbol{P}\boldsymbol{A},\quad \boldsymbol{U}=\boldsymbol{A}^{\mathrm{T}}\boldsymbol{P}(\boldsymbol{l}+\boldsymbol{\Delta}) \tag{8}$$

$$\hat{\boldsymbol{V}}=\boldsymbol{A}\delta\hat{\boldsymbol{X}}+(\boldsymbol{l}+\boldsymbol{\Delta})=\boldsymbol{R}(\boldsymbol{l}+\boldsymbol{\Delta}),\quad \boldsymbol{R}=\boldsymbol{E}-\boldsymbol{A}(\boldsymbol{A}^{\mathrm{T}}\boldsymbol{P}\boldsymbol{A})\boldsymbol{A}^{\mathrm{T}}\boldsymbol{P} \tag{9}$$

If no cycle slips exist, i. e., $\boldsymbol{\Delta}=\boldsymbol{0}$, the observation equations are only affected by random errors. The corrections (residuals) vector $\hat{\boldsymbol{V}}$ will be very small and its fluctuations will be near to zero. Fig. 3 depicts the behaviour of the corrections for a sample of data collected on a vehicle test.

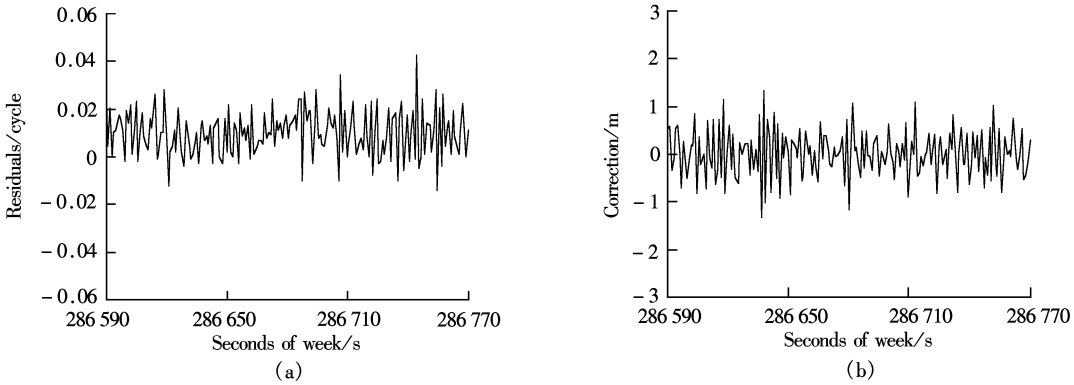

Fig. 3 Variation of corrections with no cycle slips. (a) Residuals vector $\hat{\boldsymbol{V}}$; (b) Corrections vector $\delta\hat{\boldsymbol{X}}$

We simulated cycle slips for this data. These slips were multiplied by -1 or $+1$ every 30 epochs and added to the original data. Obviously, a cycle slip of the same values of cycles occurs in all the satellites observations, in other words, all satellite-receivers' distances are changed by the same value, these effects will be absorbed in the corrections $\delta\hat{\boldsymbol{X}}$, and cannot be reflected by the residuals $\hat{\boldsymbol{V}}$. As the value of $\delta\hat{\boldsymbol{X}}$ is at the level of 1 to 3 m, only slips are large enough to be exposed by $\delta\hat{\boldsymbol{X}}$.

On the other hand, if all the satellites observations are affected by different values of cycle slips, the corrections $\delta\hat{\boldsymbol{X}}$ will only absorb the part whose effects are the same for every satellite's observation, the remainder can be reflected by the residuals $\hat{\boldsymbol{V}}$. Fig. 4 shows the behaviour of the corrections, where all satellites' observations had added slips with the value changing 1 to 6 cycles.

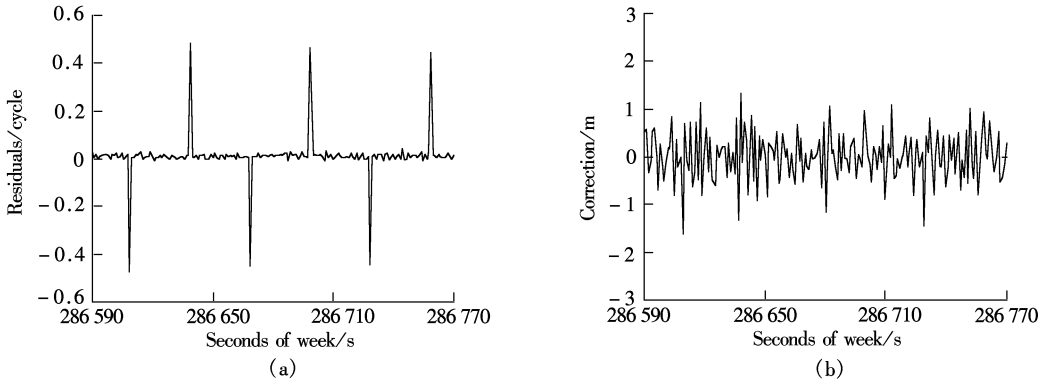

Fig. 4 Variation of corrections with all the satellites' observations affected by different value cycle slips. (a) Residuals vector $\hat{\boldsymbol{V}}$; (b) Corrections vector $\delta\hat{\boldsymbol{X}}$

As has been experienced, cycle slips can be calculated accurately by adding the parameters in Eq. (7), if four satellites' observations are not affected by cycle slips. In Fig. 5(a) we plotted the residuals computed from simulated measurements by adding slips (1 cycle) to satellite 31. And Fig. 5(b) is the estimation of the slip's parameter.

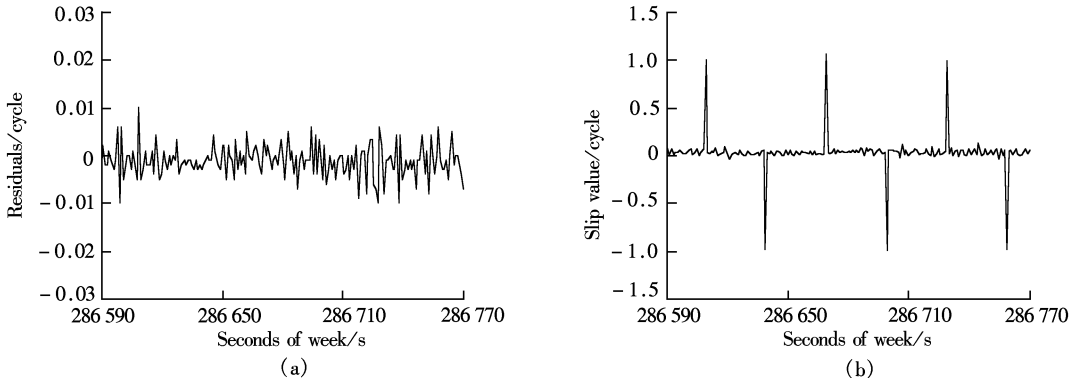

Fig. 5 Correction and estimation with the occurrence of cycle slips of one satellite's observations. (a) Residuals of satellite 31; (b) Estimation of cycle slips

If the number of unknown parameters is larger than that of L1 phase observations, pseudo-range observables must be used. As pseudo-range measurements are low accuracy, the system cannot detect small cycle slips. If dual-frequency observables are available, cycle slips can be calculated accurately by adding the parameters in Eq. (7) when four satellites observations are not affected by cycle slips. The behavior of the estimation of the slip's parameter computed from simulated measurements by adding slips (1 cycle) to L1 frequency while L2 measurements are clear is exactly the same as that in Fig. 5(b).

4 Further Discussion on Cycle Slip Detection

In GPS literature, nearly all the methods use the same strategy to detect cycle slips: processing the measurements like Eqs. (7) to (9), a smooth test quantity is obtained and the quantity will jump if a cycle slip occurs. Then one or more satellites' observations are deleted and the quantity is computed again. The deleted satellites' observations are labeled those to be affected by cycle slips if the new quantity's jump is not over a threshold. In fact, this strategy has great disadvantages, however, up to now, no literature has mentioned it.

Tab. 1 to Tab. 3 are L1 phase observation residuals. They show that the residuals computed from the measurements where all satellites' observations are affected by the same values of cycle slips are equal to cycle-slip-free case. It also shows residuals increase when slips value increases. And the effects of cycle slips are not revealed by residuals, which are adjusted by the matrix $\boldsymbol{R}$ in Eq. (9) and satellite-receiver geometry.

Tab. 1 Residuals of a cycle slips of one cycle occuring with the increase of numbers of satellites cycle

Affected satellites	Slip value	Satellites					
		31	27	11	02	08	03
No		0.002	0.008	−0.001	−0.050	0.042	−0.001
31		−0.236	0.358	−0.094	−0.090	−0.102	0.164
31, 27		0.115	−0.184	0.047	0.090	0.011	−0.080
31 to 11	1	0.021	−0.042	0.010	0.055	−0.029	−0.015
31 to 02		−0.019	0.138	−0.025	−0.536	0.424	0.018
31 to 08		−0.163	0.252	−0.066	−0.083	−0.054	0.114
All		0.002	0.008	−0.001	−0.050	0.042	−0.001

Tab. 2 Residuals of one satellite's observations affected by the increase of slip value cycle

Slip value	Affected satellite	Satellites					
		31	27	11	02	08	03
1		−0.236	0.358	−0.094	−0.090	−0.102	0.164
2		−0.474	0.709	−0.187	−0.131	−0.246	0.329
3	31	−0.712	1.060	−0.280	−0.172	−0.390	0.494
6		−1.426	2.112	−0.560	−0.293	−0.822	0.989
12		−2.853	4.216	−1.119	−0.537	−1.687	1.980

Tab. 3 Residuals of five satellites' observations affected by the increase of slip value cycle

Slip value	Affected satellites	Satellites					
		31	27	11	02	08	03
1		−0.163	0.252	−0.066	−0.083	−0.054	0.114
2	31, 27	−0.328	0.496	−0.131	−0.117	−0.149	0.228
3	11, 02	−0.493	0.741	−0.195	−0.150	−0.245	0.343
6	08	−0.988	1.474	−0.390	−0.250	−0.532	0.686
12		−1.979	2.940	−0.779	−0.451	−1.105	1.374

In Fig. 6 we plotted the residuals computed from simulated measurements by adding slips (10 cycles) to satellite 31 and 7 cycles to satellite 27. It shows these two satellites' slips counteract each other and the time series cannot be used to detect slips. Tab. 1 also illustrates this case, which has not been discussed in GPS literature.

The first reason why slips counteract each other is that the matrix $\boldsymbol{R}$ is a rank defect matrix, which not only prevents residuals from revealing slips exactly, but also causes infinite slips vectors $\boldsymbol{\Delta}$ to make $\hat{\boldsymbol{V}} \approx \boldsymbol{0}$. The second is satellite-receiver geometry. Fig. 7 illustrates the satellite-receiver geometry. It shows that satellite 2 is very near to satellite 8, which means they have the same equivalent to satellite-receiver geometry, in other words, although there are six satellites, their functions are equal to five satellites. If satellite 2 or satellite 8 observations are deleted, the residuals will not change greatly, see Tab. 4.

Therefore, satellites 31, 27, 11 and 3 are the main satellites in the geometry. If one of them is deleted, although there are five satellites and the redundancy is one, it is still difficult to use the residuals to analyze whether slips occur or not, see Tab. 5.

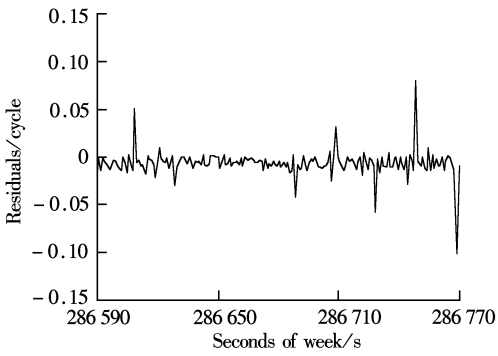

Fig. 6 Slips counteracting each other

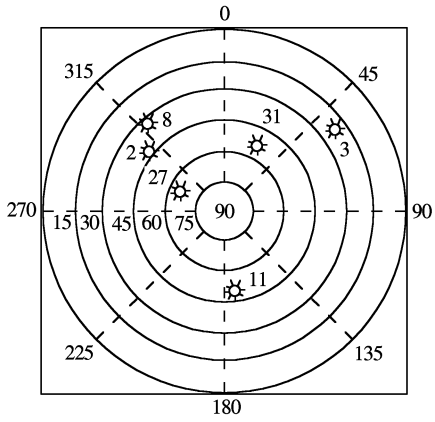

Fig. 7 Satellite-receiver geometry

Tab. 4 Residuals resulting from deleting equivalent satellites cycle

Affected satellite	Deleted satellite	Slip value	Satellites					
			31	27	11	02	08	03
			−0.091	0.149	−0.038	−0.085	0.002	0.064
11	2	1	−0.086	0.123	−0.033		−0.064	0.059
	8		−0.092	0.149	−0.038	−0.084		0.064
			−0.464	0.714	−0.187	−0.227	−0.160	0.323
11	2	5	−0.448	0.645	−0.173		−0.334	0.310
	8		−0.416	0.676	−0.173	−0.379		0.291

Tab. 5 Residuals resulting from deleting main satellites cycle

Affected satellite	Deleted satellite	Slip value	Satellites					
			31	27	11	02	08	03
			−0.091	0.149	−0.038	−0.085	0.002	0.064
	31			0.014	−0.002	−0.070	0.057	0.001
11	27	1	−0.005		−0.001	0.037	−0.034	0.003
	11		0.004	0.004		−0.049	0.043	−0.002
	03		0.001	0.012	−0.002	−0.066	0.055	
			−0.464	0.714	−0.187	−0.227	−0.160	0.323
	31			0.031	−0.005	−0.148	0.121	0.001
11	27	5	0.002		0	−0.011	0.010	−0.001
	11		0.004	0.004		−0.049	0.043	−0.002
	03		0.002	0.025	−0.004	−0.133	0.110	

5 Conclusion

The quality of GPS positioning is dependent on a number of factors. For attaining high-precision positioning results, we need to identify the main error sources impacting on the quality of the observations. In terms of data processing, cycle slips are the main sources which can deteriorate the quality of the observations and subsequently, the quality of positioning results. The detection and correction of cycle slips are needed if accurate positioning is to be carried out. Cycle slip detection and correction require the location of the jump and the determination of its size. It can be completely removed once it is correctly detected and identified. All the methods have the common premise that to detect a slip at least one smooth quantity derived from the observations must be tested in some manner for discontinuities that may represent cycle slips. Once the time series for the derived quantities have been produced, the cycle slip detection process can be initiated.

In most GPS applications, regardless of surveying modes (static and kinematic) and baseline lengths (short, medium and long), the effects of the temporal single differenced biases and noise are more or less below a few centimetres as long as the observation sampling interval is relatively short. Based on the assumption of a high sampling interval, the time-relative positioning observation equation is further analyzed, and the concept of virtual measurement is applied, which results in a stable linearization scheme. A new cycle slip detection approach based on time-relative positioning theory is studied, and valuable unrecognized knowledge of relation between satellites geometry and cycle slip detection is obtained.

References

[1] Lichtenegger H, Hofmann-Wellenhof B. GPS-data preprocessing for cycle-slip detection [A]. In: Bock Y, Leppard N, eds. *International Association of Geodesy Symposia on Global Positioning System: An Overview* [C]. Edinburgh, Scotland, 1989. 57 – 68.

[2] Bisnath S B. Efficient, automated cycle-slip correction of dual-frequency kinematic GPS data [A]. In: *Proceedings of ION GPS* 2000 [C]. Salt Lake City, Utah, 2000. 145 – 154.

[3] Bastos L, Landau H. Fixing cycle slips in dual-frequency kinematic GPS-applications using Kalman filtering [J]. *Manuscripta Geodaetica*, 1988, **13**(4): 249 – 256.

[4] Blewitt G. An automatic editing algorithm for GPS data [J]. *Geophysical Research Letters*, 1990, **17**(3): 199 – 202.

[5] Gao Y, Li Z. Cycle slip detection and ambiguity resolution algorithms for dual-frequency GPS data processing [J]. *Marine Geodesy*, 1999, **22**(4): 169 – 181.

[6] Collin F, Warnant R. Application of the wavelet transform for GPS cycle slip correction and comparison with Kalman filter [J]. *Manuscripta Geodaetica*, 1995, **20**(3): 161 – 172.

[7] Michaud S, Santeree R. Time-relative positioning with a single civil GPS receiver [J]. *GPS Solutions*, 2001, **5**(2): 71 – 77.

[8] Kim D, Langley R B. Estimation of the stochastic model for long-baseline kinematic GPS applications [A]. In: *Proceedings of the Institute of Navigation* 2001 *National Technical Meeting* [C]. Long Beach, CA, USA, 2001. 586 – 595.

基于时间相对定位理论的周跳探测方法

喻国荣　　生仁军

(东南大学交通学院,南京 210096)

摘要:提出了一种有效的用于高精度 GPS 定位或导航的周跳探测方法,该方法基于动态高采样率的假设,则时间单差观测值中的各种误差很小以至可以忽略不计,且模糊度参数值应当为零,如果发生周跳,模糊度参数的估值就是周跳,所以周跳可作为未知参数加到时间相对定位方程中进行估计. 因为时间单差观测值是由同一接收机在不同位置不同历元获得的观测值,如果时间单差点位方程如同传统测站单差方程那样线性化,将导致设计矩阵秩亏,为获得稳定的线性化方案,分析了时间相对定位方程,引入了虚观测值的概念. 车载试验数据处理结果表明,基于时间相对定位理论的周跳探测方法可以探测到一周量值的周跳. 结果还显示:如果 2 颗卫星过于接近,其对站星几何图形的影响是等价的,从而给周跳探测带来困难甚至可能得出错误结论;不同卫星发生的周跳也通过站星几何图形影响周跳探测.

关键词:GPS;周跳;时间相对定位;站星几何图形

中图分类号:P228.4